

## Article

# Silver Nanoparticles Coated with Recombinant Human Epidermal Growth Factor: Synthesis, Characterization, Liberation and Anti-*Escherichia coli* Activity

Layla M. Gonzales Matushita , Luis Palomino  and Juan Carlos F. Rodriguez-Reyes \* 

Laboratory of Nanoscale and Applications—NASCA, Department of Chemical Engineering, Universidad de Ingeniería y Tecnología—UTEC, Jr. Medrano Silva 165, Barranco, Lima 15063, Peru

\* Correspondence: jcrodriguez@utec.edu.pe

**Abstract:** Epithelial tissue regeneration may be favored if the tissue receives both therapeutic agents such as recombinant human epidermal growth factor (rhEGF) and, simultaneously, antibacterial materials capable of reducing the risk of infections. Herein, we synthesized silver nanoparticles (AgNPs), which are well-known antibacterial materials, and impregnate them with rhEGF in order to study a bio-nanomaterial of potential interest for epithelial tissue regeneration. A suspension of Ag NPs is prepared by the chemical reduction method, employing sodium citrate as both a reducer and capping agent. The AgNPs suspension is mixed with a saline solution containing rhEGF, producing rhEGF-coated Ag NPs with rhEGF loadings between 0.1 and 0.4% *w/w*. ELISA assays of supernatants demonstrate that, in all studied cases, over 90% of the added rhEGF forms part of the coating, evidencing a high efficiency in impregnation. During the preparation of rhEGF-coated Ag NPs, no significant changes are observed on the nanoparticles, which are characterized by UV-Vis spectroscopy, transmission electron microscopy (TEM) and infrared spectroscopy. The liberation of rhEGF in vitro was followed for 72 h, finding that approximately 1% of rhEGF that is present is released. The rhEGF-coated AgNPs shows antibacterial activity against *E. coli*, although such activity is decreased with respect to that observed from naked AgNPs. Having confirmed the possibility of simultaneously liberating rhEGF and reducing the proliferation of bacteria, this work helps to support the use of rhEGF-loaded metallic nanoparticles for tissue regeneration.

**Keywords:** Ag nanoparticles; EGF; characterization; biomolecule; silver



**Citation:** Gonzales Matushita, L.M.; Palomino, L.; Rodriguez-Reyes, J.C.F. Silver Nanoparticles Coated with Recombinant Human Epidermal Growth Factor: Synthesis, Characterization, Liberation and Anti-*Escherichia coli* Activity. *Reactions* **2023**, *4*, 713–724. <https://doi.org/10.3390/reactions4040041>

Academic Editors: Annalisa Volpe, Caterina Gaudiuso and Maria Chiara Sportelli

Received: 4 September 2023

Revised: 16 October 2023

Accepted: 1 November 2023

Published: 15 November 2023



**Copyright:** © 2023 by the authors. Licensee MDPI, Basel, Switzerland. This article is an open access article distributed under the terms and conditions of the Creative Commons Attribution (CC BY) license (<https://creativecommons.org/licenses/by/4.0/>).

## 1. Introduction

Nanoparticles, often recognized as materials with diameters less than 100 nm, have interesting physical and chemical properties, which allow for their application in a variety of fields, including catalysis, energy, microelectronics, sensing and biomedicine [1]. Scientists have rapidly utilized the exceptional qualities of nanomaterials for diverse biological and medical applications in the last two decades, leading to the development of novel biomedical materials for drug delivery and early diagnosis [2–4].

In drug delivery, the reduced size of nanoparticles allows for their enhanced penetration into target organs. The possibility of controlling the nanoparticle size and the surface-to-volume ratio allows for control of both the stability and release rate of therapeutic agents capable of promoting the regeneration process [5,6]. Additionally, the use of nanoparticles allows for a more targeted delivery of agents, decreasing the need for repeated administrations and reducing the risks associated with treatment-related allergies [7]. Nanomaterials employed in drug delivery include polymeric and metal-based nanoparticles. Polymeric nanoparticles can shield proteins from undesirable interactions with the environment, improve protein stability, and increase the circulation time. These benefits are strongly influenced by polymer qualities such as hydrophilicity, chain length, conformation, and biocompatibility [8]. For example, efforts to develop poly(lactic-co-glycolic acid)-based

nanoparticles (PLGA NPs) for the delivery of proteins and peptides have increased in recent years, owing to the fact that peptides, in general, cannot easily be administered orally or through the skin due to their short half-lives *in vivo*. In this regard, protein and peptide medications encapsulated in PLGA nanoparticles have allowed for simpler and less painful therapies [9]. However, the intestinal absorption of the peptides could be affected by PLGA nanoparticle properties such as size, surface charge, and hydrophobicity [10]. Polymeric nanoparticles often have larger sizes than metallic nanoparticles (more than 100 nm), which may reduce their ability to be delivered to target locations within an organism [11]. Metal-based nanoparticles represent a broad group of inorganic materials whose size can be better controlled down to a few nanometers, with interesting chemical and physical properties. They include, for example, metal oxide nanoparticles, where those with magnetic properties stand out due to the possibility of directing them to target organs by applying magnetic fields. Metallic nanoparticles are mostly restricted to elements with high stability in biological media, such as those of silver, copper, and gold [12,13]. This type of nanoparticle has size-dependent chemical and electronic properties that need to be considered in order to decide how it should be used in biomedical applications [14].

Among the metallic nanoparticles, silver nanoparticles (AgNPs) have received a great deal of attention in recent years [15]. Silver has been used in medical applications since the dawn of civilization, since it has anti-inflammatory and antibacterial properties [15]. These properties are key in wound healing, and for this reason, silver is included in several formulations for skin regeneration [4,16–18]. In this sense, AgNPs offer an advantage in wound healing as they are effective against the bacteria that generate biofilms, which have long been a concern owing to their resistance to traditional antimicrobial therapy [19]. The AgNPs–bacteria interaction could be explained in multiple ways. For example, electrostatic attraction can occur between negatively charged AgNPs (for example, when anionic stabilizers such as citrate are used) and positively charged integral protein residues on the bacteria surface. Using a different approach, AgNPs have the ability to infiltrate the bacterial membrane and cause cellular inactivation through a variety of processes, including their ability to restrict cellular respiration, to delay DNA replication, and to produce reactive oxygen species (ROS) [20–23]. Because of their diversity (size, form, physical and chemical properties), AgNPs may be employed in a wide range of applications. However, concerns have arisen regarding the use of AgNPs, especially when their size is below 10 nm, due to their cytotoxicity to many human cells, long-term exposure and tendency to agglomerate inside the body [24,25]. While these concerns require additional investigations, their application carries a considerably lower risk when used externally, such as in epithelial tissue regeneration. Indeed, certain uses, such as AgNPs-based dressings for wound treatment, have been shown to be safe and effective [22,26,27].

Silver nanoparticles have been employed to deliver bioactive peptides, providing noteworthy results in tissue regeneration [28]. AgNPs can be synthesized in various sizes and shapes (spheres, rods, and tubes) by carefully controlling the synthesis conditions [4]. Furthermore, owing to their negative surface charge, they exhibit high reactivity and can be easily linked with proteins and other biomolecules [29]. In our research group, we successfully generated silver nanoparticles at high concentrations, using the chemical reduction method with silver nitrate as a silver precursor and sodium citrate as a reducing/capping agent [30]. The attachment of other molecules to these nanoparticles can be achieved in two manners: direct attachment, relying on nanoparticle–protein interactions driven by van der Waals forces [31], and indirect attachment, which involves specific chemistries, such as click reactions [3]. These strategies are designed considering the possibility of the controlled release of such agents [32,33]. Understanding the interaction between nanoparticles and proteins is critical for the safe and effective use of AgNPs. There are several approaches for studying NP–protein interactions, but the most frequent include UV-Vis spectroscopy, Fourier-transform infrared spectroscopy (FTIR), dynamic light scattering, and zeta potential analysis [34–36].

Nanotechnology has emerged as a potential solution due to its use of nanoparticles as bioactive peptides transport vectors, as well as a potential antiseptic [37]. The tissue regeneration process is aided by bioactive proteins that are carefully controlled and released by the surrounding tissue. Growth factors (GFs) and cytokines stand out among these bioactive peptides [38]. GFs are polypeptide molecules that attach to cell receptors and provide information on migration, proliferation, differentiation, survival, and secretion. The popularity of GFs in novel therapies has recently increased, because they are easy to use and have a low cost [39]. Among the molecules needed to be delivered for tissue regeneration, recombinant human epidermal growth factor (rhEGF) is key, as this biomolecule plays an important role in wound and burn healing by encouraging the growth, proliferation, differentiation, and survival of epithelial cells [39,40]. Since rhEGF works by attaching to a particular membrane receptor (EGFR), carriers must maintain stable specific binding sites and receptor affinity zones. Furthermore, when the EGF–EGFR complex is activated, it causes cellular biochemical changes that help with inflammation, wound contraction, and fibroblast proliferation. Specifically, rhEGF is a single-chain polypeptide composed of 53 amino acid residues, with a molar mass of 10 kDa that contains six cysteine residues in its structure, which generate three disulfide bridges that are required for affinity with the receptor (EGFR) to which it binds via the  $\beta$ -loop segment (specific binding site). It is critical to note that these precise binding sites, affinity zones with the receptor, and physiologically active regions must be stable for rhEGF and EGFR binding to occur properly and achieve the desired performance [41,42].

Previous studies have focused on the application of rhEGF–AgNPs in diabetes treatments [43], second-degree burns [22] and imaging [44]. The present work explores, at a more fundamental level, the interaction between rhEGF and silver nanoparticles, following potential changes in the structure of rhEGF upon interaction with AgNPs, measuring the liberation of rhEGF in a solution simulating a physiological medium, and evaluating their antibacterial properties against *E. coli*.

## 2. Experimental Section

### 2.1. Synthesis of Ag Nanoparticles and rhEGF-Coated Ag Nanoparticles

AgNPs were synthesized using an adapted version of the Frens method, which was previously published by our group [30]. In brief, 50 mL of a 1 mM AgNO<sub>3</sub> (purity of 99.8%, J.A. Elmer) solution was placed in an Erlenmeyer flask with a stir bar in the dark and heated/stirred until boiling point. Immediately, 500  $\mu$ L of a 0.189 M sodium citrate (purity of 99.9%, Movilab) solution was added, and the mixture was stirred for 20 min. The resulting AgNPs were centrifuged (Eppendorf® Centrifuge 5415 C) at 2040 RCF (relatively centrifugal force) for 30 min and later resuspended in 1.5 mL of distilled water. The silver concentration of this solution was around 3.6 g Ag/L, as determined by weighing 500  $\mu$ L of AgNPs solution dried under vacuum. Finally, AgNPs were stored at 4 °C in the dark.

For the impregnation of rhEGF to AgNPs, volumes of 15, 35, and 55  $\mu$ L of rhEGF (from *Escherichia coli* in 50 mM HEPES/ 300 mM NaCl/ 10 mM Sodium Metabisulfite/20% glycerol at pH 8.0, Dundee Cell Products) were added to vials containing 250  $\mu$ L of the solution of suspended AgNPs. Later, distilled water was added until the total volume in the three vials was 500  $\mu$ L. This resulted in rhEGF-coated AgNPs containing, approximately, 1000, 2500, and 4000 ng of rhEGF. Considering the amount of silver, the rhEGF-coated Ag NPs had loadings of roughly 0.1, 0.25 and 0.4% rhEGF. The resulting solutions were placed in a stirring plate (IKA®-Schuttler MTS 4) at 700 RPM (revolutions per minute) for 4 h. Then, rhEGF-coated AgNPs were collected by centrifugation at 2040 RCF for 30 min and resuspended in distilled water. Supernatants were stored to evaluate the loading efficiency through EGF ELISA assays (catalog # KHG0061, Thermo Fisher Scientific Inc., Waltham, MA, USA).

## 2.2. Characterization of Ag Nanoparticles and rhEGF-Coated Ag Nanoparticles

The synthesis of pure and rhEGF-coated AgNPs was achieved using UV-Visible spectroscopy with a NanoDrop 1000 Spectrophotometer (Thermo Fisher Scientific Inc.). The nanomaterial size and morphology were characterized by transmission electron microscopy (FEI Tecna F30 300 kV). The changes in rhEGF were followed using single-point attenuated total reflectance Fourier-transform infrared (ATR-FTIR) spectroscopy, performed on a Shimadzu IR Tracer-100 FTIR, with each spectrum obtained after 200 scans at a resolution of  $4\text{ cm}^{-1}$  in the spectral range  $4000\text{--}400\text{ cm}^{-1}$ .

## 2.3. rhEGF Release Experiments

For the determination of rhEGF released from AgNPs, experiments were performed in a solution containing phosphate-buffered saline (PBS, 500  $\mu\text{L}$  at pH 7.4) and bovine serum albumin (BSA, 0.1% *w/v*), compounds able to generate a medium resembling physiological conditions. The resulting products were slowly shaken at  $37\text{ }^\circ\text{C}$ . Each 24 h for 3 days, rhEGF-coated AgNPs were collected by centrifugation at 2040 RCF for 30 min and resuspended in distilled water. Supernatants were stored for evaluation.

## 2.4. Antimicrobial Assays against *E. coli*

Antibacterial tests against *E. coli* (ATCC<sup>®</sup> 8739) were performed following previous reports from our group [24]. In brief, *E. coli* (inoculated in 50 mL of Luria–Bertani (LB) medium for 24 h at  $37\text{ }^\circ\text{C}$ ) was purified and resuspended in the same medium. The resulting *E. coli* ( $8.8 \times 10^9$  CFU/mL) was diluted five-fold in LB medium. A total of 50  $\mu\text{L}$  of the fifth dilution was suspended in 1 mL of distilled sterile water supplemented with pure AgNPs and rhEGF-coated AgNPs (in different amounts of EGF, as described in Section 2.1) in the synthesis media. The suspensions were followed over 24 h through measurements of the optical density at 600 nm, since an increased optical density has been associated with the proliferation of *E. coli* [45]. In addition, suspensions of pure AgNPs and 4000 ng rhEGF-coated AgNPs in the synthesis medium and in PBS/BSA media were shaken for 5 min, and 100  $\mu\text{L}$  of the suspensions were cultured on MacConkey agar plates for 24 h. Colonies were counted on each plate, and all experiments were performed in triplicate, from which standard deviations were estimated and reported as errors in the following section.

# 3. Results and Discussion

## 3.1. Characterization of Ag Nanoparticles and rhEGF-Coated Ag Nanoparticles

The Frens method was employed to synthesize AgNPs, which resulted in nanoparticles of 5.8 nm and 68.8 nm with spherical and cylindrical shapes at high concentrations. It also provided percentages of variance throughout the synthesis reproducibility process, of 5.5%, 0.71%, and 4.3% for absorbance, maximum wavelength and FWHM values, respectively. Furthermore, when compared to typical synthesis methods, this technique yields more stable nanoparticles, as previously reported by our group [3,30]. Figure 1 shows the UV-Vis spectrum and TEM of pure AgNPs and of these nanoparticles coated with three different amounts of rhEGF (1000, 2500, and 4000 ng rhEGF). The loading effectiveness of rhEGF over AgNPs was, in all cases, over 94%, as determined from the ELISA assays (Table 1). Considering the volume and concentration of the Ag NP suspension, the nanoparticles feature loadings of  $\sim 0.11$ , 0.25, and 0.37% rhEGF.

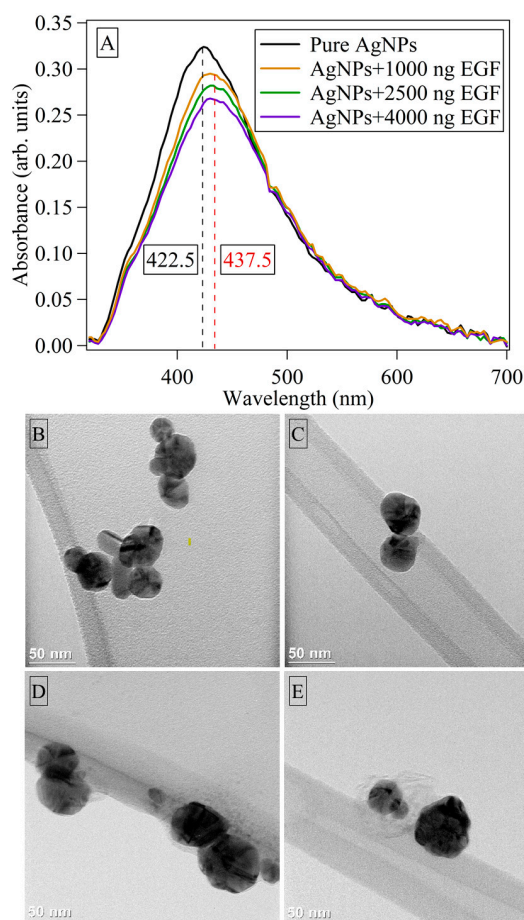


**Figure 1.** (A) UV-Vis spectra of silver nanoparticles with and without rhEGF. The concentration of Ag NPs is 33.4 mM, and later 1000, 2500, and 4000 ng of rhEGF were added. (B–E) show TEM micrographs for pure AgNPs and for 1000, 2500, and 4000 ng rhEGF-coated AgNPs, respectively.

**Table 1.** Loading efficiency (%) of rhEGF over AgNPs. Measurements were taken for the initial rhEGF solution used in synthesis and for supernatants after the interaction. For simplicity, values in the text are rounded to 1000, 2500 and 4000 ng rhEGF. The difference between these two measurements is the rhEGF loaded on AgNPs.

	rhEGF Used in Synthesis (ng)	rhEGF Loaded on AgNPs (ng)	Loading Efficiency (%)
1000 ng EGF-coated AgNPs	1061.25	1060.25	99.90
2500 ng EGF-coated AgNPs	2476.25	2456.25	99.20
4000 ng EGF-coated AgNPs	3891.25	3667.25	94.24

Figure 1A shows that, upon the addition of rhEGF, there is a *red shift* of roughly 15 nm, which is associated with an increase in the nanoparticle size due to the effective attachment of rhEGF onto the nanoparticle surface [46]. Even though the AgNPs are initially stabilized by the attachment of citrate anions to the surface [47], rhEGF is also negatively charged, since its isoelectric point (4.43) is lower than the pH of the mixing solution (close to neutral). Since the molecular weight of rhEGF is higher to that of citrate ions, the former can effectively compete for surface sites and ultimately displace citrate ions through a combination of electrostatic forces, van der Waals interactions and hydrophobic interactions [44,46,47]. We suggest that the competition for or displacement of citrate by EGF facilitates the coalescence and growth of nanoparticles, which would also lead to the decrease in absorbance as the amount of interacting rhEGF increases (Figure 1). However, it is also possible that the decrease in absorbance originates from the fact that the interaction

between rhEGF and AgNPs changes the manner in which surface plasmon electrons behave, as they become less invested in absorbing light and more invested in interacting with the rhEGF molecules [48]. The rhEGF–AgNPs interaction is evidenced by TEM images, as seen in Figure 1B–E, where, at higher concentrations of rhEGF, there is some blurriness surrounding the nanoparticles. These “clouds” correspond to rhEGF molecules coating the nanoparticle and confirm that the addition of greater amounts of rhEGF favors the attachment. The rhEGF-coated AgNPs seem to have a similar stability to pure AgNPs, as deduced from the fact that the stored nanomaterials showed only minor changes in the absorption spectra even after one week (Figure S1).

As mentioned before, ATR-FTIR has been used to investigate structural and conformational changes in proteins in order to evaluate changes in stability [36,49]. rhEGF presents three disulfide bridges (part of its tertiary structure) that are critical to its affinity for the receptor (EGFR) to which it binds via the  $\beta$ -loop segment (part of its secondary structure). Since the interaction between rhEGF and AgNPs may modify these structures, a structural examination of the polypeptide is required to assess its potential functionality and efficacy of usage. The secondary structure of proteins and polypeptides can be followed by FTIR, specifically observing changes at the amide I region (from  $1700\text{ cm}^{-1}$  to  $1600\text{ cm}^{-1}$ ) [42,50], which is shown in Figure 2A. While no bands were observed in pure AgNPs, there was a rise in absorbance strength for the bands centered at  $1681\text{ cm}^{-1}$ ,  $1666\text{ cm}^{-1}$ ,  $1649\text{ cm}^{-1}$ ,  $1635\text{ cm}^{-1}$  and  $1618\text{ cm}^{-1}$  as the amount of rhEGF was increased. The second derivative of the FTIR spectra (Figure 2B) more clearly shows the changes that occurred upon the addition of rhEGF. Larger absorbance intensity values are expected at higher levels of rhEGF, as more loop structures and beta sheets are present (even though IR spectroscopy is not a quantitative technique, qualitative changes can be deduced). Previous studies have shown that the greater the amount of rhEGF loaded on nanoparticles, the stronger the rhEGF–rhEGF interaction that is established, resulting in fewer changes in its structure [50]. Furthermore, the presence of loop structures and  $\beta$ -sheets would imply better adherence of the rhEGF to the NPs, resulting in greater polypeptide stability. Since the secondary structure of rhEGF is maintained, it is also likely that the tertiary structure remains unchanged, which would be an important advantage for the application of rhEGF-coated nanoparticles in tissue regeneration, where the ability of rhEGF to bind to its receptor is key [42,51]. Additionally, because the loop structures are preserved throughout the interaction, the  $\beta$ -loop segment as well as the disulfide bridges may retain their stability and polypeptide maintains its biological activity. Since further confirmation of the stability of rhEGF upon impregnation lies beyond the aim of the present study, we focus next on studying the possibility of liberating rhEGF.

### 3.2. Release of rhEGF

By using EGF Elisa assays, the total amount of rhEGF (ng) released from 1000, 2500, and 4000 ng rhEGF-coated AgNPs (concentration of 3.6 g/L) was measured over the course of three days. It is important to highlight that these experiments were conducted in a medium containing ions usually present in physiological medium; therefore, the results could be taken as a representative of what would happen in a real application. It is also important to note that the temperature and pH value utilized in these experiments ( $37\text{ }^{\circ}\text{C}$  and 7.4, respectively) may have an effect on the quantity of rhEGF that is released. Previous studies have found that the cumulative release of EGF occurs in an increasing sequence at any pH value [52]; therefore, it may be concluded that the interactions between rhEGF and AgNPs (van der Waals, electrostatic and hydrophobic) are the most critical elements influencing rhEGF release. The rhEGF release was monitored in the supernatants at 12, 24, 48, and 72 h (Table 2 and Figure 3). As expected, the amount of rhEGF released is greater as the rhEGF load increases. However, it is important to consider that the released rhEGF released 2% of the 1000 ng rhEGF-coated AgNP, while, for both the 2500 ng and 4000 ng rhEGF-coated AgNPs, the amount that is released accounts for  $\sim$ 1% of rhEGF. In the previous section, it was mentioned that higher loadings may promote stronger

rhEGF–rhEGF interactions; the fact that liberation is proportionally higher for 1000 ng rhEGF-Ag NPs seems to confirm this fact. The attempts to fit the data to simple first-, second-, or zero-order reactions were not successful, which suggests that liberation is a complex process or that the liberation of rhEGF follows various stages.

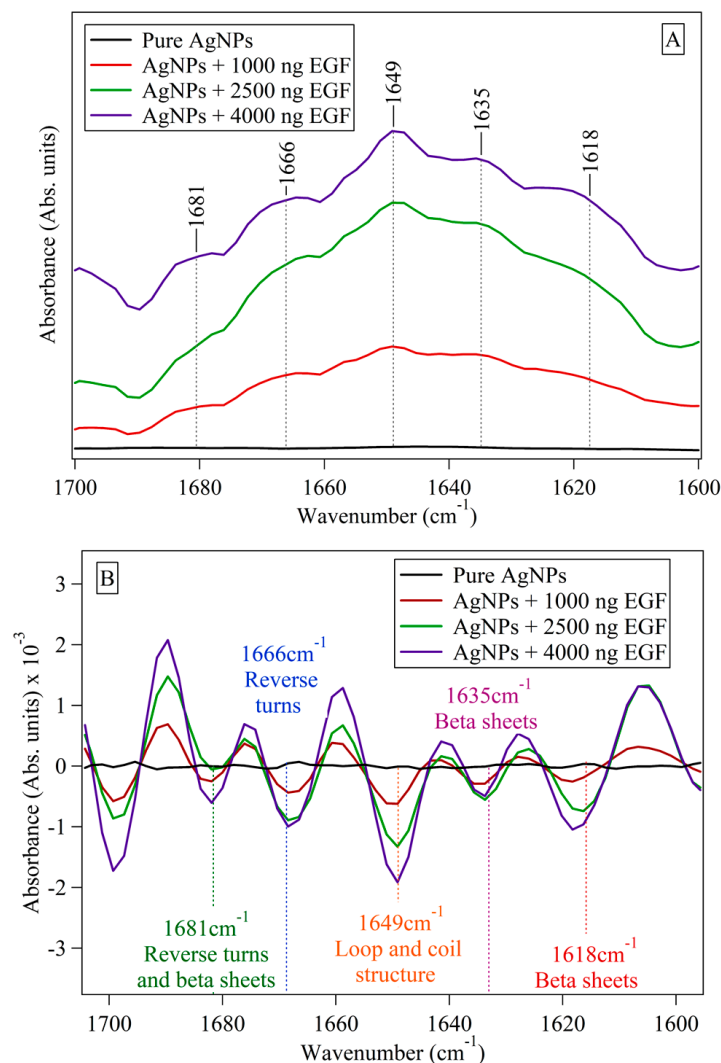


**Figure 2.** (A) FTIR spectra of the amide I region for pure AgNPs and rhEGF-coated AgNPs. (B) Second derivative of the FTIR spectra of the amide I region for pure AgNPs and rhEGF-coated AgNPs.

**Table 2.** Release of rhEGF-coated AgNPs during 72 h, expressed in nanograms and in parenthesis, as a percentage of the initial loading for each case.

Time (hours)	1000 ng EGF-Coated AgNPs	2500 ng EGF-Coated AgNPs	4000 ng EGF-Coated AgNPs
12	7.77 (0.777%)	11.66 (0.466%)	21.6 (0.54%)
24	12.77 (1.277%)	19.98 (0.799%)	34.82 (0.87%)
48	17.91 (1.791%)	26.31 (1.052%)	41.95 (1.048%)
72	20.24 (2.024%)	26.59 (1.063%)	46.7 (1.166%)

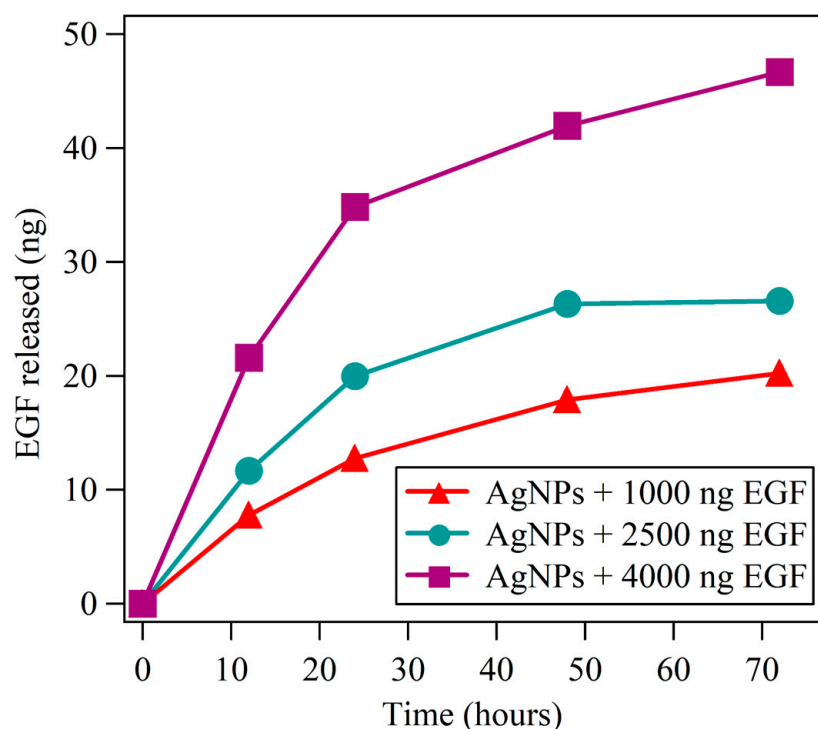


**Figure 3.** rhEGF release (ng) from rhEGF-coated AgNPs at 12, 24, 48, and 72 h. Liberation experiments were conducted in a physiological medium, as described in the text.

### 3.3. Antimicrobial Assays Using *E. coli*

The activity of AgNPs and rhEGF-coated AgNPs was first explored using the optical density of 600 nm as a guide for suspensions of *E. coli* with the addition of AgNPs with different amounts of rhEGF (See Section 2.4). These experiments showed a decrease in the optical density (which is associated with a decrease in the growth of *E. coli*) in the presence of pure AgNPs and of rhEGF-coated AgNPs (Figure 4). Even though this is an indirect guide, it is interesting to notice that the smaller rhEGF loadings (1000 and 2500 ng) yield optical densities very close to that of pure Ag NPs, while the 4000 ng rhEGF-coated AgNPs yield greater optical densities. This suggests that small rhEGF loadings do not affect the antibacterial capabilities of AgNPs, but greater loadings interfere with the antibacterial mechanisms. A likely explanation for the decreased antibacterial activity for greater rhEGF loadings is that rhEGF attaches strongly to the nanoparticle, stabilizing it and impeding the release of silver ions and the subsequent generation of reactive oxygen species.

For preparing cultures and testing the activity towards *E. coli*, only 4000 ng rhEGF-coated AgNPs were chosen, since this loading indicated differences with respect to pure Ag NPs in Figure 4. Figure 5 shows the antibacterial activity of 200 g/mL AgNPs and 4000 ng rhEGF-coated AgNPs against *E. coli* in synthesis and physiological media after 72 h. When compared to pure AgNPs, rhEGF-coated AgNPs exhibit a decrease in antibacterial activity in both media, confirming the results from Figure 4 and the conclusion that the rhEGF coating facilitates the stabilization of Ag NPs and, consequently, reduces their antibacterial efficacy. It is interesting to notice that both AgNPs and rhEGF-coated AgNPs display lower antibacterial activity in the physiological medium. While this may be attributed to the coalescence and formation of larger AgNPs in a saline environment [31,45], it is worth considering that this environment may inactivate the generation and/or activity of Ag<sup>+</sup> ions.

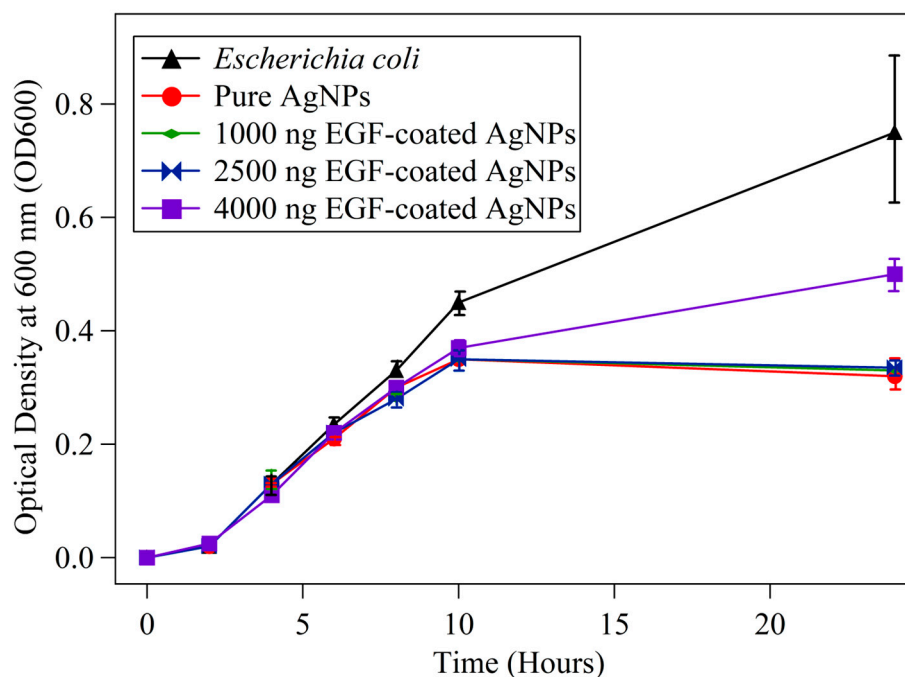


**Figure 4.** Optical density at 600 nm (OD600) of *Escherichia coli* during interaction with pure AgNPs and 1000, 2500, and 4000 ng rhEGF-coated AgNPs.

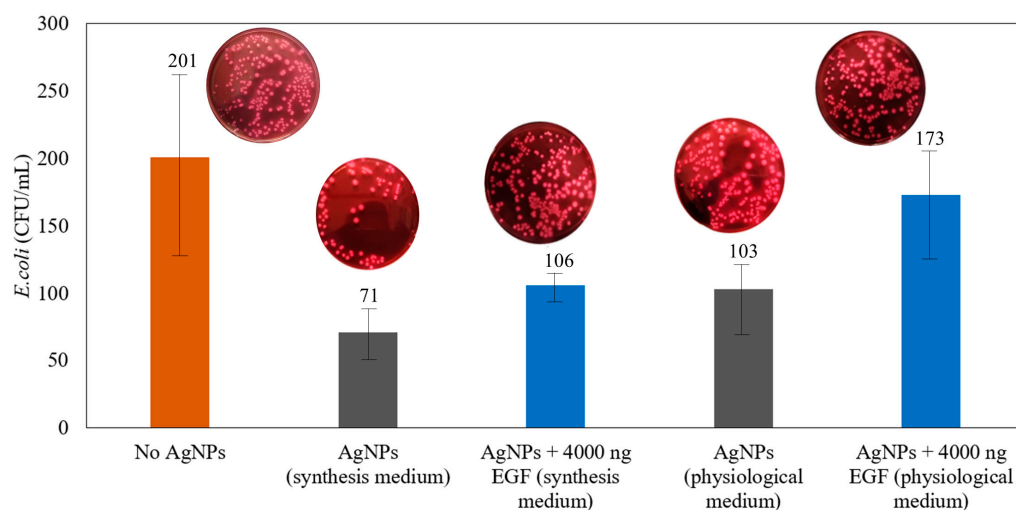


**Figure 5.** Growth of *E. coli* in the presence of pure AgNPs and 4000 rhEGF-coated AgNPs in synthesis medium and physiological medium.

#### 4. Summary and Conclusions

The present work demonstrates that rhEGF can be attached to silver nanoparticles in a straightforward manner, without significantly altering the nanoparticle size or the structure of the polypeptide. rhEGF loadings achieved in this work account for 0.1–0.4% of the total weight of the rhEGF-loaded AgNPs, with an efficiency of attachment of over 94%, as determined by ELISA assays. The formation of rhEGF-AgNPs bio-nanomaterials was demonstrated by UV-Vis, where the interaction between rhEGF and silver nanoparticles generates changes in the spectra, and by TEM, where rhEGF can be observed surrounding AgNPs at higher loadings. Furthermore, rhEGF-coated AgNPs were found to remain stable even after 7 days after synthesis. The structure of rhEGF upon interactions with AgNPs was followed by FTIR, finding evidence of the stability of the  $\beta$ -loop and of the disulfide bridges, both necessary for the biological activity of the peptide. The liberation of rhEGF in

a medium resembling physiological conditions for 72 h was in the range 1–2%, depending on the loading of rhEGF. Further research is needed to evaluate if greater loadings of rhEGF result in a more facile liberation. In anti-*Escherichia coli* essays, the rhEGF-loaded Ag NPs were observed to retain the antimicrobial activity of AgNPs for small rhEGF loadings, while the highest tested loading indicated a decrease in the antimicrobial activity. Experiments conducted in a medium containing ions present in physiological conditions showed a decrease in the antimicrobial activity in all cases, possibly due to the passivation or stabilization of AgNPs. Even though this work shows that rhEGF-coated AgNPs are bio-nanomaterials capable of liberating rhEGF and working as an antimicrobial agent, further work regarding the effect of AgNPs' size and shape, the enhancement of rhEGF liberation and the elucidation of rhEGFs' structure upon liberation is needed. In addition, tests in conditions closer to those found in a physiological environment will be needed to corroborate the results reported in this work.

**Supplementary Materials:** The following supporting information can be downloaded at: <https://www.mdpi.com/article/10.3390/reactions4040041/s1>, Figure S1: UV-Vis spectra of pure AgNPs and 1000 ng, 2500 ng and 4000 ng EGF-coated AgNPs as synthesized and after seven days, demonstrating the stability of our separation/storing methods.

**Author Contributions:** Conceptualization, L.P. and J.C.F.R.-R.; methodology, L.P. and J.C.F.R.-R.; validation, L.P., L.M.G.M. and J.C.F.R.-R.; formal analysis, L.P., L.M.G.M. and J.C.F.R.-R.; investigation, L.P., L.M.G.M. and J.C.F.R.-R.; resources, J.C.F.R.-R.; data curation, L.P., L.M.G.M. and J.C.F.R.-R.; writing—original draft preparation, L.P., L.M.G.M. and J.C.F.R.-R.; writing—review and editing, L.M.G.M. and J.C.F.R.-R.; visualization, L.M.G.M.; supervision, J.C.F.R.-R.; project administration, J.C.F.R.-R.; funding acquisition, J.C.F.R.-R. All authors have read and agreed to the published version of the manuscript.

**Funding:** This research was funded by FONDECYT—Consejo Nacional de Ciencia, Tecnología e Innovación Tecnológica (Contract number 155-2015) and by the UTEC Faculty Grants to promote international exploratory collaborative research with Cleveland Clinic (Grant number 819003) and with Harvard University (Grant number 819051).

**Data Availability Statement:** The data presented in this study are available on request from the corresponding author.

**Acknowledgments:** Julio Valdivia, Javier Paino, Marco Málaga, Ana Luisa Alvarez, Vijay Krishna and Anand Ramamurthi are thanked for their support during the development of the project. The EGF sample used in this work was generously donated by Robin Dickinson, to whom we express our gratitude. Karinna Visurraga and Luz Pérez are acknowledged for administrative support.

**Conflicts of Interest:** The authors declare no conflict of interest.

## References

1. Mobasser, S.; Firoozi, A. Review of Nanotechnology Applications in Science and Engineering. *J. Civ. Eng. Urban* **2016**, *6*, 84–93.
2. Zhang, L.; Webster, T.J. Nanotechnology and nanomaterials: Promises for improved tissue regeneration. *Nano Today* **2009**, *4*, 66–80. [[CrossRef](#)]
3. Gakiya-Teruya, M.; Palomino-Marcelo, L.; Pierce, S.; Angeles-Boza, A.M.; Krishna, V.; Rodriguez-Reyes, J.C.F. Enhanced antimicrobial activity of silver nanoparticles conjugated with synthetic peptide by click chemistry. *J. Nanopart. Res.* **2020**, *22*, 90. [[CrossRef](#)]
4. Choudhury, H.; Pandey, M.; Lim, Y.Q.; Low, C.Y.; Lee, C.T.; Marilyn, T.C.L.; Loh, H.S.; Lim, Y.P.; Lee, C.F.; Bhattamishra, S.K.; et al. Silver nanoparticles: Advanced and promising technology in diabetic wound therapy. *Mater. Sci. Eng. C* **2020**, *112*, 110925. [[CrossRef](#)]
5. Parani, M.; Lokhande, G.; Singh, A.; Gaharwar, A.K. Engineered Nanomaterials for Infection Control and Healing Acute and Chronic Wounds. *ACS Appl. Mater. Interfaces* **2016**, *8*, 10049–10069. [[CrossRef](#)]
6. Chen, L.; Yu, G.; Chu, Y.; Zhang, J.; Hu, B.; Zhang, X. Effect of three types of surfactants on fabrication of Cu-coated graphite powders. *Adv. Powder Technol.* **2013**, *24*, 281–287. [[CrossRef](#)]
7. Li, J.; Lu, Y. Protein Nanocapsule Based Protein Carriers for Industrial and Medical Applications. UCLA. 2015. Available online: <https://escholarship.org/uc/item/93k6h4dh> (accessed on 20 September 2023).
8. Gauthier, M.A.; Klok, H.A. Polymer-protein conjugates: An enzymatic activity perspective. *Polym. Chem.* **2010**, *1*, 1352–1373. [[CrossRef](#)]

9. Mundargi, R.C.; Babu, V.R.; Rangaswamy, V.; Patel, P.; Aminabhavi, T.M. Nano/micro technologies for delivering macromolecular therapeutics using poly(D,L-lactide-co-glycolide) and its derivatives. *J. Control. Release* **2008**, *125*, 193–209. [CrossRef]
10. Jung, T.; Breitenbach, A.; Kissel, T. Sulfobutylated poly(vinyl alcohol)-graft-poly(lactide-co-glycolide)s facilitate the preparation of small negatively charged biodegradable nanospheres. *J. Control. Release* **2000**, *67*, 157–169. [CrossRef]
11. Jung, T.; Kamm, W.; Breitenbach, A.; Kaiserling, E.; Xiao, J.X.; Kissel, T. Biodegradable nanoparticles for oral delivery of peptides: Is there a role for polymers to affect mucosal uptake? *Eur. J. Pharm. Biopharm.* **2000**, *50*, 147–160. [CrossRef]
12. Mody, V.; Siwale, R.; Singh, A.; Mody, H. Introduction to metallic nanoparticles. *J. Pharm. Bioallied Sci.* **2010**, *2*, 282. [CrossRef] [PubMed]
13. Mandal, D.; Bolander, M.E.; Mukhopadhyay, D.; Sarkar, G.; Mukherjee, P. The use of microorganisms for the formation of metal nanoparticles and their application. *Appl. Microbiol. Biotechnol.* **2006**, *69*, 485–492. [CrossRef] [PubMed]
14. Khursheed, R.; Dua, K.; Vishwas, S.; Gulati, M.; Jha, N.K.; Aldhafeeri, G.M.; Alanazi, F.G.; Goh, B.H.; Gupta, G.; Paudel, K.R.; et al. Biomedical applications of metallic nanoparticles in cancer: Current status and future perspectives. *Biomed. Pharmacother.* **2022**, *150*, 112951. [CrossRef] [PubMed]
15. Mathur, P.; Jha, S.; Ramteke, S.; Jain, N.K. Pharmaceutical aspects of silver nanoparticles. *Artif. Cells Nanomed. Biotechnol.* **2018**, *46*, 115–126. [CrossRef] [PubMed]
16. Chaudhury, K.; Kumar, V.; Kandasamy, J.; RoyChoudhury, S. Regenerative nanomedicine: Current perspectives and future directions. *Int. J. Nanomed.* **2014**, *9*, 4153–4167. [CrossRef] [PubMed]
17. Zarrintaj, P.; Moghaddam, A.S.; Manouchehri, S.; Atoufi, Z.; Amiri, A.; Amirkhani, M.A.; Nilforoushadeh, M.A.; Saeb, M.R.; Hamblin, M.R.; Mozafari, M. Can regenerative medicine and nanotechnology combine to heal wounds? the search for the ideal wound dressing. *Nanomedicine* **2017**, *12*, 2403–2422. [CrossRef]
18. Xie, H.-Q. Detection, biological effectiveness, and characterization of nanosilver-epidermal growth factor sustained-release carrier. *Afr. J. Pharm. Pharmacol.* **2013**, *7*, 397–404. [CrossRef]
19. Hamdan, S.; Pastar, I.; Drakulich, S.; Dikici, E.; Tomic-Canic, M.; Deo, S.; Daunert, S. Nanotechnology-Driven Therapeutic Interventions in Wound Healing: Potential Uses and Applications. *ACS Cent. Sci.* **2017**, *3*, 163–175. [CrossRef]
20. Sharma, V.K.; Yngard, R.A.; Lin, Y. Silver nanoparticles: Green synthesis and their antimicrobial activities. *Adv. Colloid Interface Sci.* **2009**, *145*, 83–96. [CrossRef]
21. Agnihotri, S.; Mukherji, S.; Mukherji, S. Size-controlled silver nanoparticles synthesized over the range 5–100 nm using the same protocol and their antibacterial efficacy. *RSC Adv.* **2014**, *4*, 3974–3983. [CrossRef]
22. Li, S.; Liu, Y.; Huang, Z.; Kou, Y.; Hu, A. Efficacy and safety of nano-silver dressings combined with recombinant human epidermal growth factor for deep second-degree burns: A meta-analysis. *Burns* **2021**, *47*, 643–653. [CrossRef] [PubMed]
23. Dror-Ehre, A.; Mamane, H.; Belenkova, T.; Markovich, G.; Adin, A. Silver nanoparticle-E. coli colloidal interaction in water and effect on E. coli survival. *J. Colloid Interface Sci.* **2009**, *339*, 521–526. [CrossRef] [PubMed]
24. Liao, C.; Li, Y.; Tjong, S.C. Bactericidal and Cytotoxic Properties of Silver Nanoparticles. *Int. J. Mol. Sci.* **2019**, *20*, 449. [CrossRef]
25. Dos Santos, C.A.; Seckler, M.M.; Ingle, A.P.; Gupta, I.; Galdiero, S.; Galdiero, M.; Gade, A.; Rai, M. Silver nanoparticles: Therapeutic uses, toxicity, and safety issues. *J. Pharm. Sci.* **2014**, *103*, 1931–1944. [CrossRef]
26. Gunasekaran, T.; Nigusse, T.; Dhanaraju, M.D. Silver nanoparticles as real topical bullets for wound healing. *J. Am. Coll. Clin. Wound Spec.* **2011**, *3*, 82–96. [CrossRef] [PubMed]
27. Rigo, C.; Ferroni, L.; Tocco, I.; Roman, M.; Munivrana, I.; Gardin, C.; Cairns, W.R.L.; Vindigni, V.; Azzena, B.; Barbante, C.; et al. Active silver nanoparticles for wound healing. *Int. J. Mol. Sci.* **2013**, *14*, 4817–4840. [CrossRef] [PubMed]
28. Mordorski, B.; Rosen, J.; Friedman, A. Nanotechnology as an innovative approach for accelerating wound healing in diabetes. *Diabetes Manag.* **2015**, *5*, 329–332. [CrossRef]
29. Comfort, K.K.; Maurer, E.I.; Braydich-Stolle, L.K.; Hussain, S.M. Interference of silver, gold, and iron oxide nanoparticles on epidermal growth factor signal transduction in epithelial cells. *ACS Nano* **2011**, *5*, 10000–10008. [CrossRef]
30. Gakiya-Teruya, M.; Palomino-Marcelo, L.; Rodriguez-Reyes, J.; Gakiya-Teruya, M.; Palomino-Marcelo, L.; Rodriguez-Reyes, J.C.F. Synthesis of Highly Concentrated Suspensions of Silver Nanoparticles by Two Versions of the Chemical Reduction Method. *Methods Protoc.* **2018**, *2*, 3. [CrossRef]
31. Palomino-marcelo, L.; Gakiya, M.; Rodriguez-Reyes, J.C.F. Protocol for Studying the Interaction of Silver Nanoparticles with Biomolecules: The Case for Bovine Serum Albumin (BSA). Available online: [https://www.researchgate.net/publication/333672086\\_Protocol\\_for\\_studying\\_the\\_interaction\\_of\\_silver\\_nanoparticles\\_with\\_biomolecules\\_The\\_case\\_for\\_bovine\\_serum\\_albumin\\_BSA?channel=doi&linkId=5cfdc8f1a6fdccd1308f816f&showFulltext=true](https://www.researchgate.net/publication/333672086_Protocol_for_studying_the_interaction_of_silver_nanoparticles_with_biomolecules_The_case_for_bovine_serum_albumin_BSA?channel=doi&linkId=5cfdc8f1a6fdccd1308f816f&showFulltext=true) (accessed on 1 May 2023).
32. Venkataraman, L.; Sivaraman, B.; Vaidya, P.; Ramamurthi, A. Nanoparticulate delivery of agents for induced elastogenesis in three-dimensional collagenous matrices. *J. Tissue Eng. Regen. Med.* **2014**, *12*, 181–204. [CrossRef]
33. Sivaraman, B.; Ramamurthi, A. Multifunctional nanoparticles for doxycycline delivery towards localized elastic matrix stabilization and regenerative repair. *Acta Biomater.* **2013**, *9*, 6511–6525. [CrossRef] [PubMed]
34. Pareek, V.; Bhargava, A.; Bhanot, V.; Gupta, R.; Jain, N.; Panwar, J. Formation and Characterization of Protein Corona Around Nanoparticles: A Review. *J. Nanosci. Nanotechnol.* **2018**, *18*, 6653–6670. [CrossRef] [PubMed]
35. Del Pino, P.; Pelaz, B.; Zhang, Q.; Maffre, P.; Nienhaus, G.U.; Parak, W.J. Protein corona formation around nanoparticles—From the past to the future. *Mater. Horiz.* **2014**, *1*, 301–313. [CrossRef]

36. Kong, J.; Yu, S. Fourier transform infrared spectroscopic analysis of protein secondary structures. *Acta Biochim. Biophys. Sin. (Shanghai)* **2007**, *39*, 549–559. [[CrossRef](#)] [[PubMed](#)]
37. Ikada, Y. Challenges in tissue engineering. *J. R. Soc. Interface* **2006**, *3*, 589–601. [[CrossRef](#)]
38. Cabrera, C.; Carriquiry, G.; Pierinelli, C.; Reinoso, N.; Arias-Stella, J.; Paino, J.E. The role of biologically active peptides in tissue repair using umbilical cord mesenchymal stem cells. *Ann. N. Y. Acad. Sci.* **2012**, *1270*, 93–97. [[CrossRef](#)]
39. Krafts, K.P. Tissue repair: The hidden drama. *Organogenesis* **2010**, *6*, 225–233. [[CrossRef](#)]
40. Cross, M.; Dexter, T.M. Growth factors in development, transformation, and tumorigenesis. *Cell* **1991**, *64*, 271–280. [[CrossRef](#)]
41. Ogiso, H.; Ishitani, R.; Nureki, O.; Fukai, S.; Yamanaka, M.; Kim, J.H.; Saito, K.; Sakamoto, A.; Inoue, M.; Shirouzu, M.; et al. Crystal structure of the complex of human epidermal growth factor and receptor extracellular domains. *Cell* **2002**, *110*, 775–787. [[CrossRef](#)]
42. Yang, C.H.; Wu, P.C.; Huang, Y.B.; Tsai, Y.H. A new approach for determining the stability of recombinant human epidermal growth factor by thermal fourier transform infrared (ftir) microspectroscopy. *J. Biomol. Struct. Dyn.* **2004**, *22*, 101–110. [[CrossRef](#)]
43. Skóra, B.; Szychowski, K.A. Molecular mechanism of the uptake and toxicity of EGF-LipoAgNPs in EGFR-overexpressing cancer cells. *Biomed. Pharmacother.* **2022**, *150*, 113085. [[CrossRef](#)] [[PubMed](#)]
44. Lucas, L.J.; Tellez, C.; Castilho, M.L.; Lee, C.L.D.; Hupman, M.A.; Vieira, L.S.; Ferreira, I.; Raniero, L.; Hewitt, K.C. Development of a sensitive, stable and EGFR-specific molecular imaging agent for surface enhanced Raman spectroscopy. *J. Raman Spectrosc.* **2015**, *46*, 434–446. [[CrossRef](#)]
45. Gnanadhas, D.P.; Ben Thomas, M.; Thomas, R.; Raichur, A.M.; Chakravorty, D. Interaction of silver nanoparticles with serum proteins affects their antimicrobial activity in vivo. *Antimicrob. Agents Chemother.* **2013**, *57*, 4945–4955. [[CrossRef](#)] [[PubMed](#)]
46. Banerjee, V.; Das, K.P. Interaction of silver nanoparticles with proteins: A characteristic protein concentration dependent profile of SPR signal. *Colloids Surfaces B Biointerfaces* **2013**, *111*, 71–79. [[CrossRef](#)] [[PubMed](#)]
47. Kim, N.A.; Lim, D.G.; Lim, J.Y.; Kim, K.H.; Jeong, S.H. Fundamental analysis of recombinant human epidermal growth factor in solution with biophysical methods. *Drug Dev. Ind. Pharm.* **2015**, *41*, 300–306. [[CrossRef](#)] [[PubMed](#)]
48. Gan, X.; Liu, T.; Zhong, J.; Liu, X.; Li, G. Effect of silver nanoparticles on the electron transfer reactivity and the catalytic activity of myoglobin. *ChemBioChem* **2004**, *5*, 1686–1691. [[CrossRef](#)]
49. Dasgupta, N.; Ranjan, S.; Patra, D.; Srivastava, P.; Kumar, A.; Ramalingam, C. Bovine serum albumin interacts with silver nanoparticles with a “side-on” or “end on” conformation. *Chem. Biol. Interact.* **2016**, *253*, 100–111. [[CrossRef](#)]
50. Bhattacharjee, T.T.; Castilho, M.L.; de Oliveira, I.R.; Jesus, V.P.S.; Hewitt, K.C.; Raniero, L. FTIR study of secondary structure changes in Epidermal Growth Factor by gold nanoparticle conjugation. *Biochim. Biophys. Acta-Gen. Subj.* **2018**, *1862*, 495–500. [[CrossRef](#)]
51. Tetenbaum, J.; Miller, L.M. A new spectroscopic approach to examining the role of disulfide bonds in the structure and unfolding of soybean trypsin inhibitor. *Biochemistry* **2001**, *40*, 12215–12219. [[CrossRef](#)]
52. Banerjee, I.; Mishra, D.; Das, T.; Maiti, T.K. Wound pH-responsive sustained release of therapeutics from a poly(NIPAAm-co-AAc) hydrogel. *J. Biomater. Sci. Polym. Ed.* **2012**, *23*, 111–132. [[CrossRef](#)]

**Disclaimer/Publisher’s Note:** The statements, opinions and data contained in all publications are solely those of the individual author(s) and contributor(s) and not of MDPI and/or the editor(s). MDPI and/or the editor(s) disclaim responsibility for any injury to people or property resulting from any ideas, methods, instructions or products referred to in the content.